Landscape patterns shape wetland pond ecosystem function from glacial headwaters to ocean

Carmella Vizza [1]*, Jacob A. Zwart,[1] Stuart E. Jones [1], Scott D. Tiegs,[2] Gary A. Lamberti[1]

[1]Department of Biological Sciences, University of Notre Dame, Notre Dame, Indiana
[2]Department of Biological Sciences, Oakland University, Rochester, Michigan

Abstract

Examining patterns and processes along the aquatic continuum from headwaters to ocean can benefit from a landscape ecology approach, where hydrologic and ecological processes depend on landscape position. We conducted a study of freshwater wetland ponds subject to similar climatic conditions but distributed along a 20-km trajectory from glacial headwaters to ocean in southcentral Alaska, U.S.A. Specifically, we investigated how proximity to glaciers and ocean influenced physical, chemical, and biological characteristics of ponds. Physicochemical patterns along a distance gradient from the ocean supported the hypothesized influence of elevation and potential atmospheric deposition of marine-derived nitrogen, whereas those related to glacial flow path length may reflect inputs from glacial weathering. We expected that the effects of landscape and hydrology on physicochemical patterns would provide a template for shaping ecosystem processes, but ecosystem processes also appeared to contribute to physicochemical patterns across this landscape. Ponds more heavily influenced by glaciers tended to be more heterotrophic exhibiting greater rates of organic-matter decomposition and ecosystem respiration, which were positively correlated with phosphorus and iron concentrations likely due to glacial weathering and remineralization processes. In contrast, ponds near the ocean tended to be more autotrophic exhibiting greater gross primary production and net ecosystem production, processes that may have contributed to greater total nitrogen, nitrogen to phosphorus ratios, and dissolved organic carbon concentrations. Consideration of the relative importance of hydrologic inputs across the landscape is needed because the acceleration of glacial melt and sea-level rise by climate change may alter future broad-scale patterns of ecosystem processes.

Landscape ecology aims to explore spatial and temporal patterns across heterogeneous landscapes and to examine their influences on biotic and abiotic processes (Risser 1987; Turner 2005). The exploration of these patterns is a classical theme in aquatic ecology. For example, the "River Continuum Concept," a foundation for many studies in stream ecology, posits that the varying conditions along a river from headwaters to the mouth shape its chemical and biological processes (Vannote et al. 1980). Similarly, limnologists have documented the influence of landscape position (e.g.,

elevation or lake network number) on the chemical and biological properties of lakes (Kratz et al. 1997; Soranno et al. 1999; Sadro et al. 2011). Landscape patterns can therefore affect physical, chemical, and biological aspects of aquatic ecosystems.

Hydrology is particularly important in shaping landscape patterns in both rivers and lakes. For example, headwater streams tend to be dominated by inputs of coarse particulate organic matter (e.g., leaves and woody debris) from the surrounding forest, but downstream where the channel widens, the influence of the forest declines and primary producers within the stream (e.g., algae and aquatic plants) begin to play a larger role (Vannote et al. 1980). The "River Continuum Concept" thereby relates the physics and hydrology of flowing waters to their biological characteristics (e.g., invertebrate and fish diversity) and ecosystem processes (i.e., the relative importance of production vs. respiration). Similarly in lakes, landscape position or elevation can determine the relative importance of precipitation, runoff, and groundwater inputs, which in turn shape pH, dissolved organic carbon

*Correspondence: cvizza@nd.edu

(DOC), nutrient availability, and base cation concentrations (Kratz et al. 1997; Soranno et al. 1999; Sadro et al. 2011). While studies of landscape position relate hydrology to chemical and biological characteristics of lakes such as fish species richness (Kratz et al. 1997), chlorophyll (Soranno et al. 1999), and bacterioplankton abundance (Sadro et al. 2011), very few studies have directly examined the landscape influences on ecosystem processes. One exception is Kling et al. (2000) who found that lake primary productivity tended to decrease lower in the landscape likely due to the corresponding decreases in particulate carbon and nitrogen. Therefore, hydrology and its influence on a landscape can shape both chemical and biological patterns as well as ecosystem processes in aquatic ecosystems.

Proximity to hydrologic sources, such as the ocean, can also play an important role in shaping chemical and biological processes. For example, in estuarine systems of the Chesapeake Bay, Jordan et al. (2008) observed that as salinity and pore-water sulfate availability increased, pore-water concentrations of dissolved iron and ammonium decreased, while dissolved inorganic phosphorus increased, thereby exhibiting lower N : P ratios. They hypothesized that the mechanism behind these patterns was geological and that these patterns could contribute to the shift from nitrogen limitation in coastal marine water to phosphorus limitation in freshwater (Jordan et al. 2008). Additionally, we might expect that freshwater systems closer to the ocean would tend to exhibit higher sulfate due to sea spray and marine atmospheric deposition (Junge and Werby 1958). Because of the ocean's potential influence on both atmospheric and aquatic chemistry, it is reasonable to assume that these changes in nutrient stoichiometry could also affect ecosystem processes across the landscape (e.g., Vitousek et al. 1997; Simó and Pedrós-Alió 1999).

Proximity to glaciers could also alter chemical and biological processes of freshwater ecosystems. For example, phosphorus availability in glacially influenced Alaskan rivers peaked when runoff was highest due to glaciated watersheds having higher yields of phosphorus, which tend to be associated with poorly weathered calcite/apatite-rich minerals (Hood and Scott 2008). Additionally, glacially influenced streams of the Copper River, Alaska, receive high loads of suspended sediment and colloidal iron associated with silicates because of the physical processes of mechanical weathering (Schroth et al. 2011). Because glacier-fed streams tend to have higher turbidity, lower temperatures, and therefore less suitable habitat for algae and invertebrates than groundwater-fed streams (Malard et al. 2006), one might expect that glacially influenced aquatic ecosystems may tend toward heterotrophy rather than autotrophy.

Although past research demonstrates that oceanic and glacial inputs can affect their respective aquatic ecosystems, we know less about how these influences interact in a single broad-scale landscape (O'Neel et al. 2015). The Copper River Delta (CRD) in southcentral Alaska is a unique landscape that allows us to examine the interactive influences of both ocean and glaciers across an aquatic continuum. To examine the glacier-to-ocean continuum, we surveyed physicochemical properties and ecosystem function in 15 freshwater ponds. We hypothesized that landscape position would strongly influence physicochemical properties in these ponds, which in turn would affect ecosystem processes such as organic-matter decomposition and ecosystem metabolism. Because glacially influenced systems may be less suitable for primary and secondary producers (Malard et al. 2006) and headwaters generally tend to exhibit greater heterotrophy (Vannote et al. 1980), we also hypothesized that the relative importance of heterotrophic vs. autotrophic processes would increase closer to the glaciers and decrease closer to the ocean.

Methods

Study area

The CRD in southcentral Alaska is a heterogeneous landscape bounded by the Chugach and Wrangell Mountains to the north and the Gulf of Alaska to the south. Seven large glaciers dominate the landscape, with the Childs and Miles glaciers feeding the Copper River during the spring. The Copper River watershed has 22% glacial cover, or 14,084 km^2 of glacial area, with 69% of its regional runoff coming from glaciers (Neal et al. 2010). The immense amount of glacial sediment that pours into the Gulf of Alaska from the Copper River can be seen from satellite images (Fig. 1). Specifically, the Copper River comprises 15% of the Gulf of Alaska basin area contributing about 8% of its runoff. In addition to being the eighth largest river in the United States, the Copper River and its sediment deposits have given rise to the largest contiguous wetland on the Pacific Coast of North America (U.S. Geological Survey 1990). The CRD encompasses about 283,000 hectares of habitat, which support high biodiversity (Bryant 1991) in a relatively pristine landscape. This landscape was altered by the Great Alaska earthquake of 1964, which elevated the CRD by 1–4 m depending on location, thereby creating and modifying numerous wetland ponds (Thilenius 1995). Since the earthquake, the CRD has been subsiding at a rate of approximately 8.5 mm per year (Freymueller et al. 2008). A natural succession of aquatic habitats thereby emerges from the glaciers to the ocean of which our study focuses on 15 freshwater ponds (Fig. 1; Table 1).

The hydrology of the CRD landscape is complex with the ponds being surrounded by channels of the Copper River, smaller streams originating from nearby glaciers, and sloughs that drain tidewater and the wetlands (Tiegs et al. 2013*b*). Across the CRD, there are two predominant landscape types, outwash plain and uplifted marsh (Boggs 2001). Outwash plains are shaped by sediment from glacial streams, while the uplifted marsh landscape is formerly tidal marsh that was elevated above tidal influence by the 1964 earthquake
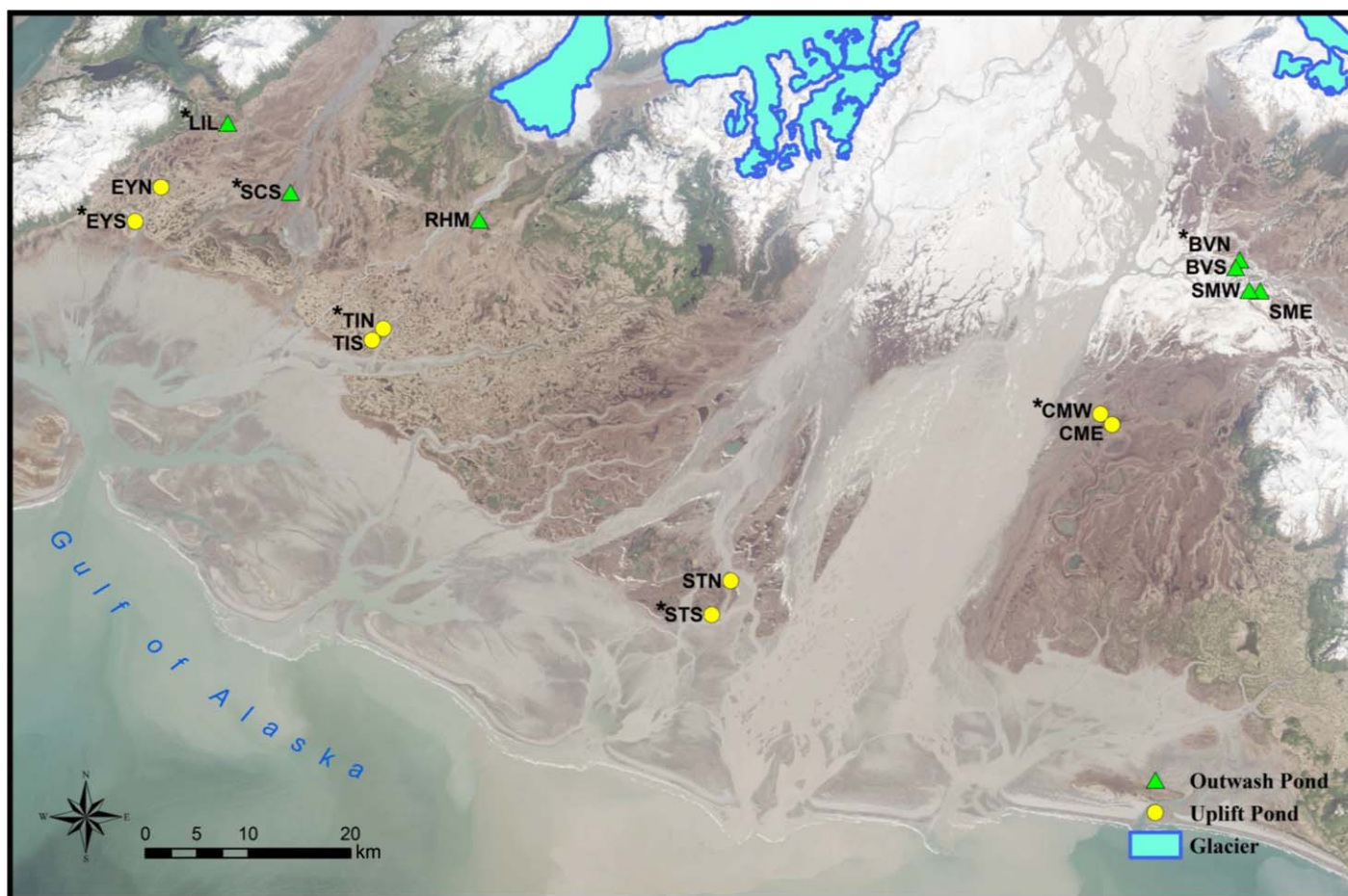
Fig. 1. Map of the CRD depicting the ponds designated as study sites (*n* = 15). Ponds on the glacial outwash plain are marked with triangles, ponds uplifted during the Great Alaska earthquake of 1964 are marked with circles, and ponds where ecosystem metabolism measurements were conducted are marked with asterisks. This map was made using Landsat 8 imagery acquired on 28 May 2013, courtesy of NASA Goddard Space Flight Center and U.S. Geological Survey. Points depicting pond locations are the geographic center of each pond and do not represent pond size. Glacier features are from the USGS National Hydrography Dataset Waterbody feature type *Ice Mass*. The map was projected using the NAD 1983 Alaska Albers projection.

(Boggs 2001). Although all ponds in this study are non-tidal freshwater ecosystems, the surrounding slough channels closest to the ocean experience tidal influence. Additionally, the proximity of CRD ponds to the ocean could result in physicochemical patterns that reflect atmospheric deposition (Bergström et al. 2005) or former marine sediments (e.g., D'Amore et al. 2011). In addition to oceanic influence, these ponds may receive glacial input via surface runoff from glacier-fed streams or subsurface groundwater flow, but their inferred primary hydrologic source is precipitation (Luca Adelfio, U.S.D.A. Forest Service, pers. comm.).

We sampled seven ponds located along the outwash plain and eight ponds along the uplifted marsh (Fig. 1). These 15 ponds were sampled during the summers of 2013 or 2014; the nine ponds west of the mainstem of the Copper River were sampled in summer 2013, whereas the six ponds to the east were sampled in summer 2014. Five areas representative of major habitat types in each pond were sampled repeatedly.

Physicochemical parameters

To examine landscape influences on physicochemical patterns, we measured dissolved oxygen (DO), pH, specific conductivity, and salinity in the upper water column ($\sim$ 0.1 m below the surface) at the five different sites per pond during July 2013 or 2014 using a YSI Pro Plus multiparameter water quality meter (YSI, Yellow Springs, Ohio). Water depth was also measured at each site using a stadia rod. Temperature and light were measured hourly for approximately 1 month using a HOBO Pendant Temperature Logger (Onset Computer Corporation, Bourne, Massachusetts), which was deployed in the center of each pond at a depth of 0.1 m (Table 1).

Estimates of light attenuation coefficient

We estimated daily light attenuation coefficients (KdPAR) for photosynthetically active radiation (PAR) using paired temperature sensors based on methods described in Read et al. (2015). This method is used for water bodies where

Table 1. Physicochemical parameters (mean ± SD) of the CRD ponds sampled in the summers of 2013 and 2014 including depth, daily temperature, water column light level, the coefficient of light attenuation (K_{dPAR}), pH, specific conductivity (SpC), salinity, dissolved oxygen (DO) levels, and sediment organic matter (SOM).* Ponds marked with asterisks (*) were located on the outwash plain; those unmarked were considered part of the uplifted marsh landscape.

Pond	Depth (m)	Daily temperature (°C)	Light (kilolux)	K_{dPAR} (m^{-1})	pH	SpC (μs cm^{-1})	Salinity (ppt)	DO (mg L^{-1})	SOM (%)
Beaver N (BVN)*	1.14 ± 0.02	16.1 ± 1.7	8.9 ± 18	1.3 ± 0.2	5.9 ± 0.1	20 ± 1.1	0.01	8.9 ± 0.3	2.3 ± 0.5
Beaver S (BVS)*	0.86 ± 0.08	15.5 ± 1.4	1.8 ± 4.2	1.7 ± 0.8	6.1 ± 0.2	24 ± 1.1	0.01	6.6 ± 0.3	2.6 ± 0.7
Clear Martin E (CME)	0.83 ± 0.04	15.4 ± 1.8	5.4 ± 8.4	1.1 ± 0.4	5.7 ± 0.1	52 ± 3.1	0.02	2.7 ± 0.7	2.3 ± 0.1
Clear Martin W (CMW)	0.81 ± 0.04	15.9 ± 2.3	1.7 ± 3.3	1.7 ± 0.8	7.7 ± 0.5	47 ± 1.3	0.02	10 ± 0.6	2.3 ± 0.5
Eyak N (EYN)	0.52 ± 0.04	16.6 ± 2.3	9.3 ± 12	1.2 ± 0.6	6.3 ± 0.1	9.5 ± 0.3	0.00	7.7 ± 0.5	2.9 ± 0.7
Eyak S (EYS)	0.59 ± 0.04	17.6 ± 2.6	14 ± 18	0.5 ± 0.2	6.6 ± 0.1	8.8 ± 0.2	0.00	8.3 ± 0.4	2.5 ± 0.3
Lily (LIL)*	0.61 ± 0.01	15.7 ± 2.5	6.1 ± 10	1.7 ± 0.7	7.0 ± 0.1	76 ± 11	0.04	3.7 ± 0.5	2.1 ± 0.4
Rich Hate Me (RHM)*	0.64 ± 0.12	13.6 ± 1.7	7.7 ± 11	1.3 ± 0.7	7.2 ± 0.1	81 ± 2.4	0.04	3.6 ± 1.0	7.9 ± 5.9
Scott S (SCS)*	0.89 ± 0.14	16.3 ± 2.5	11 ± 20	1.3 ± 0.6	7.4 ± 0.1	53 ± 5.0	0.02	8.2 ± 0.4	1.6 ± 0.4
Smiley E (SME)*	0.66 ± 0.02	14.9 ± 1.2	2.4 ± 4.5	2.0 ± 1.1	6.3 ± 0.2	44 ± 2.9	0.02	11 ± 0.4	3.5 ± 0.9
Smiley W (SMW)*	1.04 ± 0.05	15.6 ± 1.7	4.7 ± 10	1.1 ± 0.5	6.7 ± 0.2	70 ± 0.8	0.03	11 ± 0.5	1.9 ± 0.3
Storey N (STN)	0.57 ± 0.01	19.4 ± 2.6	13 ± 23	0.6 ± 0.4	7.6 ± 0.1	42 ± 0.4	0.02	8.5 ± 0.3	2.2 ± 0.4
Storey S (STS)	0.54 ± 0.09	19.1 ± 2.8	13 ± 19	1.9 ± 0.6	7.6 ± 0.1	63 ± 1.8	0.03	8.1 ± 0.5	2.1 ± 1.1
Tiedeman N (TIN)	0.60 ± 0.03	18.3 ± 2.6	12 ± 21	0.7 ± 0.6	6.6 ± 0.1	11 ± 0.6	0.00	6.2 ± 1.1	2.3 ± 0.1
Tiedeman S (TIS)	0.73 ± 0.04	18.1 ± 2.7	14 ± 23	0.8 ± 0.8	6.6 ± 0.1	8.2 ± 0.9	0.00	7.8 ± 0.5	2.9 ± 0.9

* All parameters with the exception of the temperature, light, and K_{dPAR} were measured at five different sites per pond. DO, pH, salinity, and SpC were from spot measurements of the upper water column. Salinity did not vary by site. Temperature and light were taken hourly during the month of July.

solar radiation is the dominant source of temperature changes within the water column, ideally small water bodies with low wind shear mixing and/or high K_{dPAR}. In each of the 15 ponds, we measured water temperature at two discrete depths using a HOBO Pendant Temperature Logger (Onset Computer Corporation, Bourne, Massachusetts) at 0.1 m and either a HOBO Pendent Temperature Logger or miniDOT (Precision Management Engineering, Vista, California) at a fixed depth between 0.3 m and 0.6 m. In short, paired time series of temperature within each pond are related to each other by a linear scaling factor (α) and K_{dPAR} can be estimated from the equation $K_{dPAR} = \ln(\alpha)/(z_{deep} - z_{shallow})$. Estimates of K_{dPAR} were rejected if the coefficient of variation for α were greater than 0.20. Daily estimates of K_{dPAR} were then averaged by pond. Due to one of the temperature loggers being out of water at Eyak North in 2013, we used temperature data from 2014 to calculate K_{dPAR}, but 2013 data were used in all other analyses for this pond.

Water and sediment chemistry

To characterize physicochemical parameters of each pond, we collected 1 L of water from the upper water column at each site per pond from both July and August 2013 or 2014 ($n = 10$ per pond). Using a handheld bucket auger, sediment samples were collected from each site ($n = 5$) from each pond during July 2013 or 2014. Water samples were filtered through glass fiber filters (Whatman GF/F, 0.7 μm pore size), except for those to be processed later for total phosphorus (TP). All water and sediment samples were frozen until analysis, with the exception of samples for DOC, total nitrogen (TN), and bulk elemental measurements, which were preserved with hydrochloric acid such that sample concentration was approximately 0.13 M HCl and refrigerated until analysis.

We measured dissolved ammonium (NH_4^+) using the phenol-hypochlorite method (Solórzano 1969), nitrate (NO_3^-) using the cadmium reduction method (APHA 1995), and soluble reactive phosphorus (SRP) using the ascorbic acid method (Murphy and Riley 1962) on a Lachat Flow Injection Autoanalyzer (Lachat Instruments, Loveland, Colorado). TP was analyzed using a hydroxide and persulfate digestion (Ameel et al. 1993) followed by the ascorbic acid method for SRP (APHA 1995) using a spectrophotometer (Genesys 2, Genesys, Daly City, California). DOC measured as non-purgeable organic carbon and TN were analyzed using a Shimadzu TOC-VCSH (Shimadzu Scientific Instruments, Kyoto, Japan). Bulk elemental concentrations of calcium (Ca), iron (Fe), magnesium (Mg), manganese (Mn), potassium (K), and sodium (Na) were analyzed using a PerkinElmer Optima 8000 ICP-OES (PerkinElmer, Waltham, Massachusetts). Sulfate (SO_4^{2-}) concentrations were analyzed using a Dionex ICS-5000 (Thermo Fisher Scientific,

Sunnyvale, California). All analytes were within detection limits except for NO_3^-, for which all samples fell below 5 µg N L^{-1}; therefore dissolved inorganic nitrogen (DIN) was comprised entirely of NH_4^+ (Table 2). All water chemistry analyses were performed at the University of Notre Dame, many of which utilized instrumentation at the Center for Environmental Science and Technology.

Sediment organic matter (SOM) was measured by drying sediment for at least 48 h at 60°C, and then weighing it. Sediment was then combusted at 500°C for 4 h to incinerate organic matter. Last, the sediment was re-wetted and then dried at 60°C for at least 48 h before weighing the final time (Steinman et al. 2006). SOM was estimated as the percent of material lost during combustion (SOM%, Table 1).

Organic-matter decomposition

To evaluate decomposition rates, we deployed a cotton-strip assay (after Tiegs et al. 2007, 2013a). The cotton fabric used in the assay is highly standardized and consists of 95% cellulose. Cotton strips were placed into mesh bags with a pore size of 5 × 3 mm (Cady Bag Company, Pearson, Georgia). A total of five bags, or one per site, was placed in the benthos at each of the ponds by attaching them to conduit pipe with nylon cord. Each bag contained two replicate cotton strips prepared as detailed in Tiegs et al. (2013a) for a total of 10 strips per pond. In August 2013, we placed cotton strips in the nine ponds to the west of the Copper River and retrieved them in June 2014. In August 2014, we had originally planned to conduct decomposition assays in the six remaining ponds east of the Copper River, but Beaver North was inundated with glacial meltwater thus making this assay logistically untenable at this pond. Strips were placed in the remaining five eastern ponds and retrieved in June 2015. After removal from the ponds, cotton strips were soaked in 80% ethanol for about 30 s and lightly brushed off to remove external debris. Strips were then dried at approximately 25°C, placed in grips (Checkline, Model #G1008, Enschede, The Netherlands), and their tensile strength was measured using a tensiometer (Mark-10, Model #MG100, Copiague, New York) at a fixed rate of 2 cm min^{-1} (Tiegs et al. 2013a). Decomposition rates are reported as the percent of tensile strength lost per day during incubation, with initial tensile strength estimated from strips that were not incubated in the ponds. The replicates from each site were then averaged for further statistical analysis.

Ecosystem metabolism

Seven ponds were selected for ecosystem metabolism measurements to span the east-to-west gradient of proximity with the Copper River, while capturing both glacial outwash and uplifted sites. We collected high-frequency (60-min interval) DO and temperature data within these ponds at a fixed depth of 0.3–0.4 m using miniDOTs (Precision Management Engineering, Vista, California). Water temperature and incoming light were also logged at 0.1 m depth with HOBO

Table 2. Water column chemistry (mean ± SD) of the CRD ponds sampled in the summers of 2013 and 2014 including conservative cations (Ca, K, Mg, Na), reactive metals (Fe, Mn), sulfate (SO_4^{2-}), DOC, ammonium (NH_4^+), SRP, TN, and TP. All parameters were surface layer measurements from the five different sites per pond taken during July and August (n = 10).

Pond	Ca (mg L^{-1})	K (mg L^{-1})	Mg (mg L^{-1})	Na (mg L^{-1})	Fe (mg L^{-1})	Mn (µg L^{-1})	SO_4^{2-} (µM)	DOC (mg L^{-1})	NH_4^+ (µg N L^{-1})	SRP (µg P L^{-1})	TN (µg N L^{-1})	TP (µg P L^{-1})
BVN	2.8±1.1	0.8±0.4	0.8±0.4	0.9±0.2	1.2±1.0	18±12	39±32	2.7±1.2	1.1±1.0	3.7±1.0	130±62	27±12
BVS	2.4±0.2	1.1±0.3	0.4±0.02	0.6±0.1	0.3±0.1	4.0±2.0	19±5.4	3.6±0.8	0.9±1.0	3.2±0.9	190±33	34±14
CME	5.1±0.7	1.0±0.5	0.9±0.1	1.0±0.1	1.1±0.3	19±8.1	4.0±1.3	4.5±0.8	0.8±1.7	2.9±0.8	210±31	18±9
CMW	5.2±0.8	0.6±0.4	1.0±0.1	0.8±0.1	0.4±0.1	3.4±0.7	24±3.8	4.5±0.4	0.6±0.6	3.8±1.0	230±32	29±13
EYN	0.5±0.2	0.6±0.1	0.5±0.1	1.2±0.1	0.4±0.1	11±6.5	4.4±2.1	7.1±0.6	11±2.8	4.8±1.5	270±40	34±8
EYS	0.4±0.1	0.7±0.4	0.4±0.1	0.9±0.3	0.4±0.2	4.2±0.8	3.9±0.4	6.8±0.9	13±5.7	4.8±2.5	280±34	38±13
LIL	7.5±1.8	0.7±0.5	1.1±0.3	3.1±0.5	1.6±0.7	320±350	5.0±2.1	4.2±0.5	6.2±0.8	6.9±3.1	130±28	24±7
RHM	13±0.9	1.3±0.1	1.5±0.1	2.3±0.5	9.9±4.9	610±180	7.0±1.7	4.0±0.5	15±5.3	8.6±2.5	120±29	19±8
SCS	6.6±1.4	1.7±0.4	0.9±0.2	1.7±0.6	0.6±0.1	200±200	28±3.6	2.7±0.4	5.0±1.0	8.7±3.0	110±25	23±7
SME	4.0±0.4	1.3±0.4	0.6±0.03	0.7±0.1	0.1±0.1	3.0±1.3	60±9.3	3.8±0.3	0.5±0.5	5.1±3.3	180±32	27±9
SMW	7.7±0.9	2.2±0.3	1.0±0.1	0.8±0.2	0.2±0.1	9.1±3.2	74±8.9	2.9±0.7	0.5±0.9	4.3±2.0	160±44	27±9
STN	5.3±0.6	1.4±0.3	1.0±0.1	1.0±0.1	0.5±0.1	9.2±3.6	5.3±2.0	8.7±1.6	13±0.9	4.0±0.7	300±98	24±7
STS	9.0±0.2	1.3±0.3	1.5±0.1	1.4±0.1	0.3±0.1	7.2±2.4	6.0±1.5	5.5±1.7	15±2.6	5.6±2.1	220±89	20±7
TIN	1.0±0.3	0.8±0.5	0.5±0.1	0.6±0.1	0.7±0.1	6.3±2.6	5.1±2.2	8.0±0.4	14±2.4	5.2±1.0	250±10	31±6
TIS	0.4±0.2	0.7±0.4	0.4±0.1	0.6±0.05	0.8±0.5	4.0±1.3	3.1±1.0	6.4±0.5	11±1.1	4.8±0.9	200±22	27±5

Pendant Temperature Loggers (Onset Computer Corporation, Bourne, Massachusetts). We used wind speed data from the hourly observations at the M. K. (Mudhole) Smith Airport located centrally on the west side of the CRD to estimate gas flux across the air–water interface of each pond; these quality-controlled climatological data are supported by National Centers for Environmental Information (National Oceanic and Atmospheric Administration) with each station using an anemometer to measure wind speed at a height of approximately 1.5 m above the surface. All high-frequency data were quality-assured and controlled to remove outliers and sensor errors with the open-source software B3 (Lake Ecosystem Restoration New Zealand 2016). Data were removed when sensors were out of the water, which occurred at the ends of the deployment time periods and for the shallow logger in Eyak North pond during 2013. We estimated rates of gross primary production (GPP), ecosystem respiration (ER), and net ecosystem production (NEP = GPP − ER) by fitting a maximum likelihood metabolism model to the high-frequency DO data as described by Solomon et al. (2013). We used a bootstrapping routine to estimate uncertainty in daily metabolism, where we created 1000 boot-strapped DO time series and refit the metabolism model, creating a distribution of 1000 GPP, ER, and NEP estimates for each day. The free-water O_2 method can occasionally produce a low metabolic signal-to-noise ratio if physical rather than biological processes dominate the evolution of DO (Rose et al. 2014), resulting in uncertain estimates of metabolism. Currently, there is not a consensus as to how to deal with uncertain metabolism estimates (Winslow et al. 2016). Since we were interested in cross-pond comparisons rather than day-to-day variations in metabolism within ponds, we chose to exclude uncertain metabolism estimates that had a conservative coefficient of variation greater than 1; this occurred on 44% of the metabolism days, leaving us with 7–46 confident daily metabolism estimates for each pond with an average coefficient of variation ranging from 0.24 to 0.71. We standardized GPP and ER estimates to 20°C according to Parkhill and Gulliver (1999) and Holtgrieve et al. (2010), respectively, and NEP was standardized by subtracting ER_{20} from GPP_{20}. These seasonal means of these standardized estimates were used in all subsequent analyses.

Geographic information system (GIS) mapping and flow paths

As indicators of glacial and oceanic influence, we measured the shortest flow path length from the nearest glacier to each pond as well as the shortest geodesic distance from the ocean to each pond using ArcGIS. Shortest glacial flow path for each pond was estimated using the USGS National Hydrography Dataset *Flowline* and *Waterbody* features (U.S. Geological Survey 2013) and the *Network Analyst* toolbar in ArcMap. Specifically, *Edge Flags* were placed along the NHD Flowlines at the glacial outlet and each pond, and the *Find*

Path function was used to measure the shortest flow path distance between each pond and the nearest glacier. Shortest geodesic distance was measured using the *Measure* tool set to the geodesic distance option in ArcMap between the ocean and each pond. Features were projected in ArcMap using the NAD 1983 Alaska Albers projection.

Although our intention was to use these measurements to approximate oceanic and glacial influence, we acknowledge that they are not perfect proxies, especially on the CRD where hydrologic flow paths can be both complex and dynamic. Distance from ocean was a good indicator of landscape position due its close relationship with elevation ($r = 0.83$, $p = 0.00014$, df = 13, Table 3), whereas glacial flow path length estimates the potential of glacial input to each pond, but not necessarily the actual glacial input. In creating the metric glacial flow path length, we assumed that glacial inputs came mostly from overland flow, but it is possible that they originate from groundwater inputs (Bryant 1991) or even weather-related events like dust storms (Crusius et al. 2011). Despite our expectations that distance from ocean and glacial flow path length would be inversely related, we did not see this pattern due to the CRD's heterogeneous landscape with many glaciers ($r = -0.13$, $p = 0.65$, df = 13; Table 3; Fig. 1).

Statistical analyses

To investigate patterns and processes across the landscape, we treated each pond as an experimental unit. Physicochemical and ecosystem functional processes were therefore averaged by pond for all statistical analyses to avoid pseudoreplication in space and time. We used linear regressions to explore potential mechanistic links between patterns and processes across this landscape (e.g., Turner 2005). All statistical analyses were performed in the R software environment using the base package (R Development Core Team 2016).

To explore physicochemical gradients across the CRD, we chose 13 parameters of interest including Ca (a representative of conservative cations), Fe (a representative of reactive metals), temperature, light, pH, DOC, SO_4^{2-}, and multiple N and P parameters (NH_4^+, SRP, DIN : SRP, TN, TP, TN : TP). We then conducted linear regressions of distance from the ocean and glacial flow path length with the 13 parameters specified above. To control for false-positive results, we utilized a false discovery rate control. Unlike the traditional Bonferroni correction, which lowers α for multiple statistical tests, a false discovery rate control explicitly manages the error rate of conclusions among significant results by taking into account the distribution of the p-values and the number of tests being conducted (Glickman et al. 2014). For these analyses, we set α, or the maximum false discovery rate, to 0.05. The untransformed data used in linear regressions met parametric assumptions, except for the regression involving glacial flow path length and Fe where both variables had to be log-transformed to ensure that residuals were normally distributed (Fig. 3b). We conducted 15 linear regressions

Table 3. Landscape parameters of the CRD ponds. Distance from ocean and glacial flow path length are proxies for atmospheric influence from the ocean and hydrologic influence from the glacier, respectively.

Pond	Latitude	Longitude	Elevation (m)	Pond area (m^2)	Distance from ocean (km)	Glacial flow path length (km)
BVN	60.460	−144.716	15.2	55,443	42.3	31.0
BVS	60.458	−144.718	15.5	21,481	41.5	31.1
CME	60.390	−144.829	11.0	667,059	24.7	44.4
CMW	60.393	−144.837	9.8	85,594	25.3	44.3
EYN	60.492	−145.661	5.2	6670	8.3	27.0
EYS	60.477	−145.683	5.5	6636	4.1	32.7
LIL	60.520	−145.601	8.2	20,536	17.3	19.4
RHM	60.478	−145.382	18.3	3571	18.2	6.4
SCS	60.491	−145.547	13.4	10,369	10.9	18.7
SME	60.448	−144.698	16.8	39,476	38.6	30.7
SMW	60.448	−144.707	15.8	26,648	38.1	31.0
STN	60.323	−145.161	4.6	151,748	1.5	64.7
STS	60.306	−145.178	2.1	177,486	0.2	67.1
TIN	60.431	−145.466	5.5	6768	4.0	15.3
TIS	60.425	−145.473	5.5	57,003	2.5	16.8

with a false discovery rate control for each functional process (i.e., decomposition, ER, GPP, and NEP) to determine whether the physicochemical ($n = 13$) or landscape parameters (distance from ocean and glacial flow path length; $n = 2$) influenced ecosystem function.

Results

### Oceanic and glacial influence on physicochemical patterns

Physicochemical parameters varied across the landscape (Tables 1, 2) with distinctive oceanic and glacial patterns emerging. Surprisingly, SO_4^{2-} concentrations in ponds increased with distance from the ocean (Fig. 2a). In contrast, light, temperature, DOC, NH_4^+, and DIN : SRP decreased the farther ponds were from the ocean (Fig. 2b–f). The amount of water column light was negatively correlated with its light attenuation coefficient ($r = -0.65$, $p = 0.0089$, df $= 13$). The ratio of DIN to SRP tended to be driven by NH_4^+ ($r = 0.91$, $p < 0.0001$, df $= 13$), and not SRP ($r = 0.05$, $p = 0.87$, df $= 13$). In contrast, TN : TP significantly increased with glacial flow path length (Fig. 3a), with TN ($r = 0.70$, $p = 0.0036$, df $= 13$) exerting stronger control over this pattern than TP ($r = -0.29$, $p = 0.30$, df $= 13$). Additionally, Fe decreased significantly with longer glacial flow path, but this pattern was primarily driven by the pond (Rich Hate Me) nearest a glacier (Fig. 3b). To investigate this pattern further, we also examined the relationship between Fe (log-transformed) relative to the amount of Ca and Mg (meq L^{-1}), a proxy for groundwater input (Kratz et al. 1997), and found that they were not significantly correlated ($r = 0.41$, $p = 0.13$, df $= 13$).

Because it appeared that Fe was not solely due to pond groundwater inputs, we also investigated whether glacial flow path length influenced the amount of Fe relative to groundwater input (Fe : Ca + Mg). We found that ponds with shorter glacial flow paths had greater Fe concentrations relative to hypothesized groundwater input (Fig. 3c). In addition to Fe, SRP also tended to decrease with longer glacial flow paths, albeit not significantly (Fig. 3d).

Relationships between ecosystem function and physicochemical patterns

Landscape patterns in physicochemical parameters were associated with changes in ecosystem processes. Faster decomposition rates were associated with higher SRP concentrations in the water column (Fig. 4a). Additionally, decomposition rates tended to be highest in ponds with lower TN : TP ratios, although this relationship was not significant after applying the false discovery rate control (Fig. 4b). Interestingly, SRP and TP concentrations were not significantly correlated in the ponds ($r = -0.32$, $p = 0.25$, df $= 12$), suggesting a tight relationship between decomposition and inorganic nutrients.

Despite the smaller number of ponds sampled ($n = 7$), interesting trends emerged in ecosystem metabolism. For example, ER tended to decrease with glacial flow path length (Fig. 5a), and therefore tended to increase with Fe, an indicator of glacial influence (Fig. 5b). In addition, GPP tended to be higher in ponds with higher DOC and TN concentrations (Fig. 5c,d), with DOC and TN being highly correlated in these ecosystems ($r = 0.88$, $p < 0.0001$, df $= 13$). Overall, NEP significantly decreased with higher Fe concentrations (Fig.
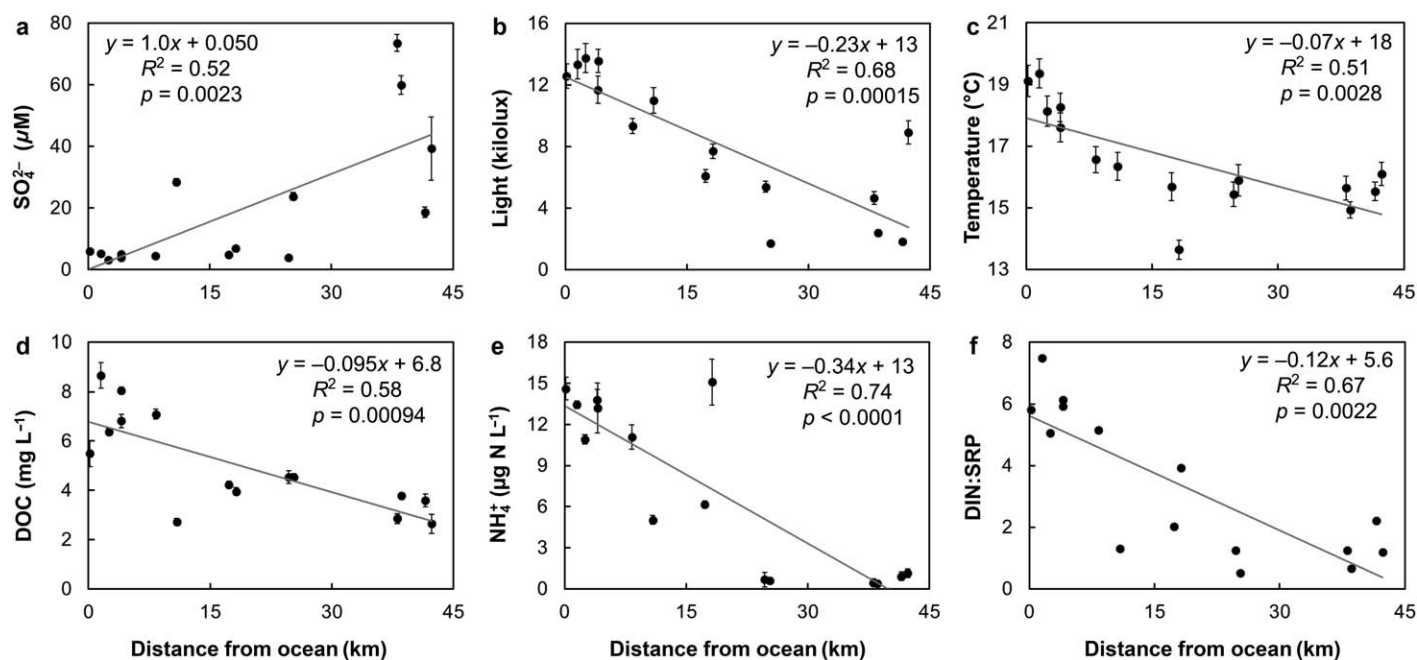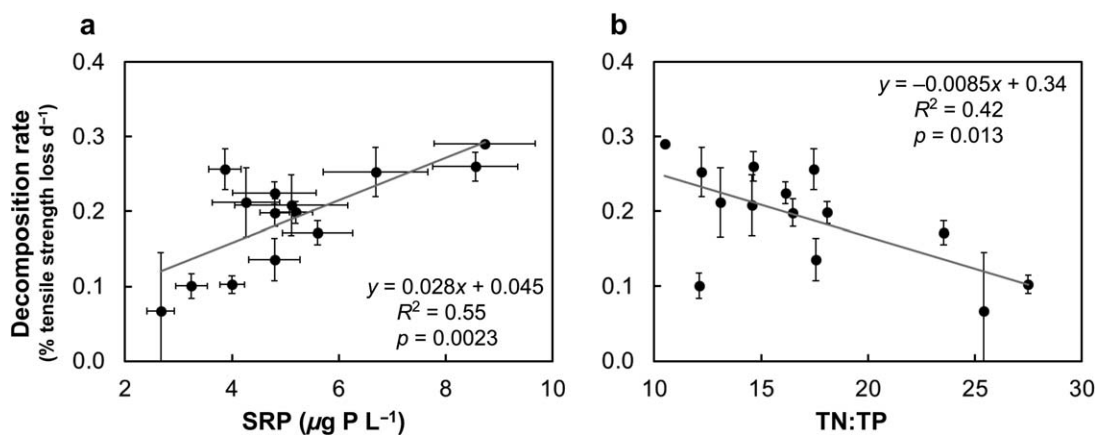
Fig. 2. Linear regressions (df = 13) between a pond's distance from the ocean and its physicochemical parameters, specifically, (**a**) sulfate (SO_4^{2-}), (**b**) water column light level, (**c**) temperature, (**d**) DOC, (**e**) ammonium (NH_4^+), and (**f**) DIN to SRP ratios. Water column nitrate measurements were below detection limit (5 μg N L^{-1}), and were therefore considered 0 in DIN calculations. DIN : SRP is reported as a molar ratio. p values greater than 0.01 were not considered significant due to the false discovery rate control cutoff. Error bars represent standard error of measurements conducted at multiple sites within a pond during summer sampling.
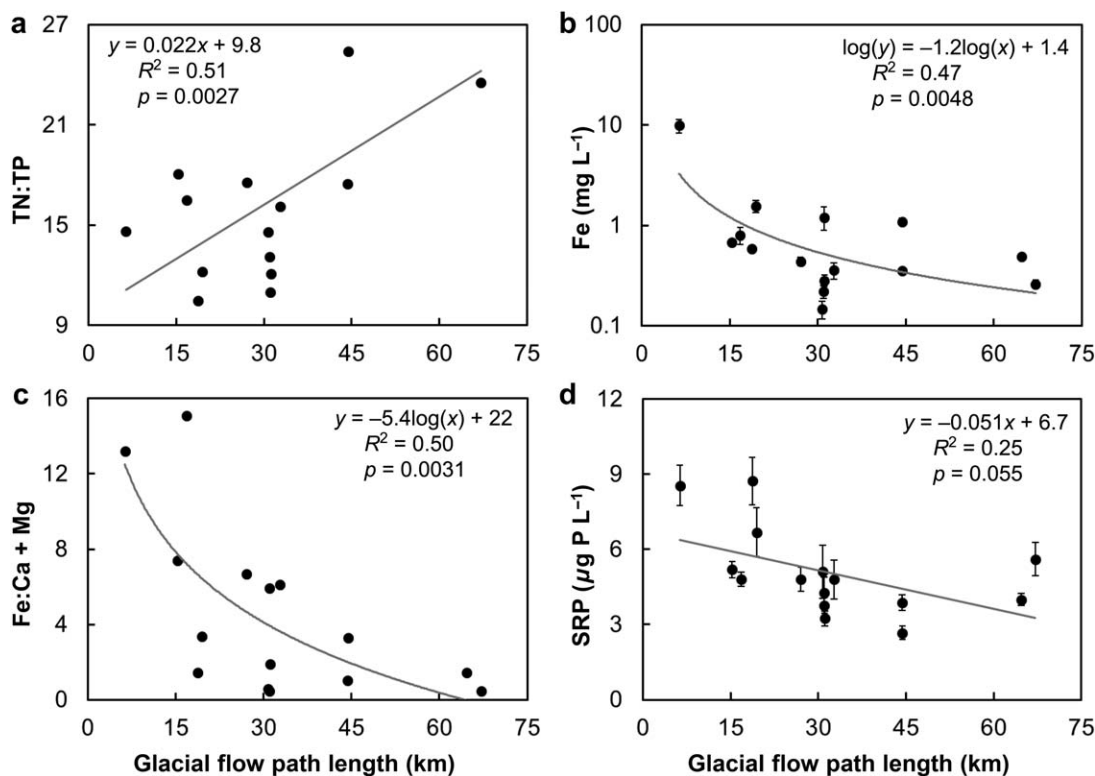
Fig. 3. Linear regressions (df = 13) between a pond's glacial flow path and its physicochemical parameters, specifically, (**a**) TN to TP levels, (**b**) iron (Fe), (**c**) Fe (mg L^{-1}) relative to hypothesized groundwater inputs (Ca + Mg, meq L^{-1}), and (**d**) SRP. TN : TP is reported as a molar ratio. p values greater than 0.01 were not considered significant due to the false discovery rate control cutoff. Error bars represent standard error of measurements conducted at multiple sites within a pond during summer sampling.

Fig. 4. Linear regressions (df = 12) between decomposition rates of cotton strips deployed in ponds and their water column nutrient concentrations, specifically, (**a**) SRP and (**b**) TN to TP levels. TN : TP is reported as a molar ratio. *p* values greater than 0.007 were not considered significant due to the false discovery rate control cutoff. Error bars represent standard error of measurements conducted at multiple sites within a pond during summer sampling.

5e), and tended to be higher in ponds with higher TN : TP ratios, albeit not significantly (Fig. 5f).

Discussion

Distinct physicochemical patterns emerged across the landscape from glaciers to ocean of these non-tidal Alaska freshwater ponds. Patterns along a distance gradient from the glaciers supported the inferred influence of inputs from glacial weathering, while proximity to the ocean likely reflected atmospheric deposition and transition to autotrophic processes. Although the landscape likely acts as a hydrologic template for physicochemical patterns, ecosystem processes also play an important role in shaping these patterns. Heterotrophic processes dominated near the glaciers and were correlated with Fe and P concentrations, likely due to glacial weathering and greater remineralization of these nutrients with decomposition and ER. In contrast, ponds closer to the ocean exhibited relatively greater autotrophy and GPP, with the higher biological production likely generating higher TN and DOC concentrations. The balance of autotrophic and heterotrophic processes also appeared to be influenced by varying N : P ratios, which increased with proximity to the ocean.

Glacial influence on physicochemical patterns and ecosystem processes

Longer glacial flow paths were associated with higher TN : TP ratios in the CRD ponds, and we suspect this relationship resulted from internal nutrient cycling processes that were largely driven by the nitrogen cycle. TN in CRD ponds reflects the concentration of inorganic nitrogen (which was greater near the ocean), the amount of organic nitrogen contributed from catchment vegetation during runoff, and internal nitrogen cycling by phytoplankton and

aquatic macrophytes. Soranno et al. (1999) and Sadro et al. (2011) both found that TN tended to increase lower in the landscape due to greater inputs of runoff associated with surrounding catchment vegetation. While this mechanism could contribute to the pattern we observed in TN : TP ratios, our data suggest that TN in these ponds largely reflects the nitrogen pool of its primary producers (i.e., macrophyte exudates and possibly phytoplankton) because DOC, TN, and GPP are tightly coupled in these ecosystems.

In addition to N : P ratios, glacial flow path length was also linked to Fe concentrations. Although Fe can be a tracer of glacial input (Bryant 1991; Crusius et al. 2011), the species and class of particulate iron likely varies with the complex hydrogeology of the CRD (Schroth et al. 2011). Schroth et al. (2011) found that mechanical weathering in glacially influenced streams resulted in higher amounts of colloidal iron associated with silicates, whereas biological processes (e.g., redox processing and iron complexation with humic acids from decomposition) in boreal-forested streams resulted in higher amounts of Fe hydroxides and Fe^{3+}. We acknowledge that our bulk measurements of Fe do not capture the species or class of particulate iron; therefore, it is difficult to distinguish among the different processes suggested by Schroth et al. (2011). Nevertheless, Fe does appear to be a reasonable indicator of glacial influence for two reasons: (1) Fe was an order of magnitude greater in the pond closest to a glacier (i.e., Rich Hate Me) than in systems more than 15 km away, suggesting strong proximal influence of glaciers on Fe that diminishes with distance, and (2) the amount of Fe relative to hypothesized groundwater inputs (Ca + Mg) decreased with glacial flow path length, suggesting that glacial runoff could be a source of Fe for these ponds.

Like Fe, we also observed higher SRP concentrations in ponds with shorter glacial flow path length. Similarly, Hood
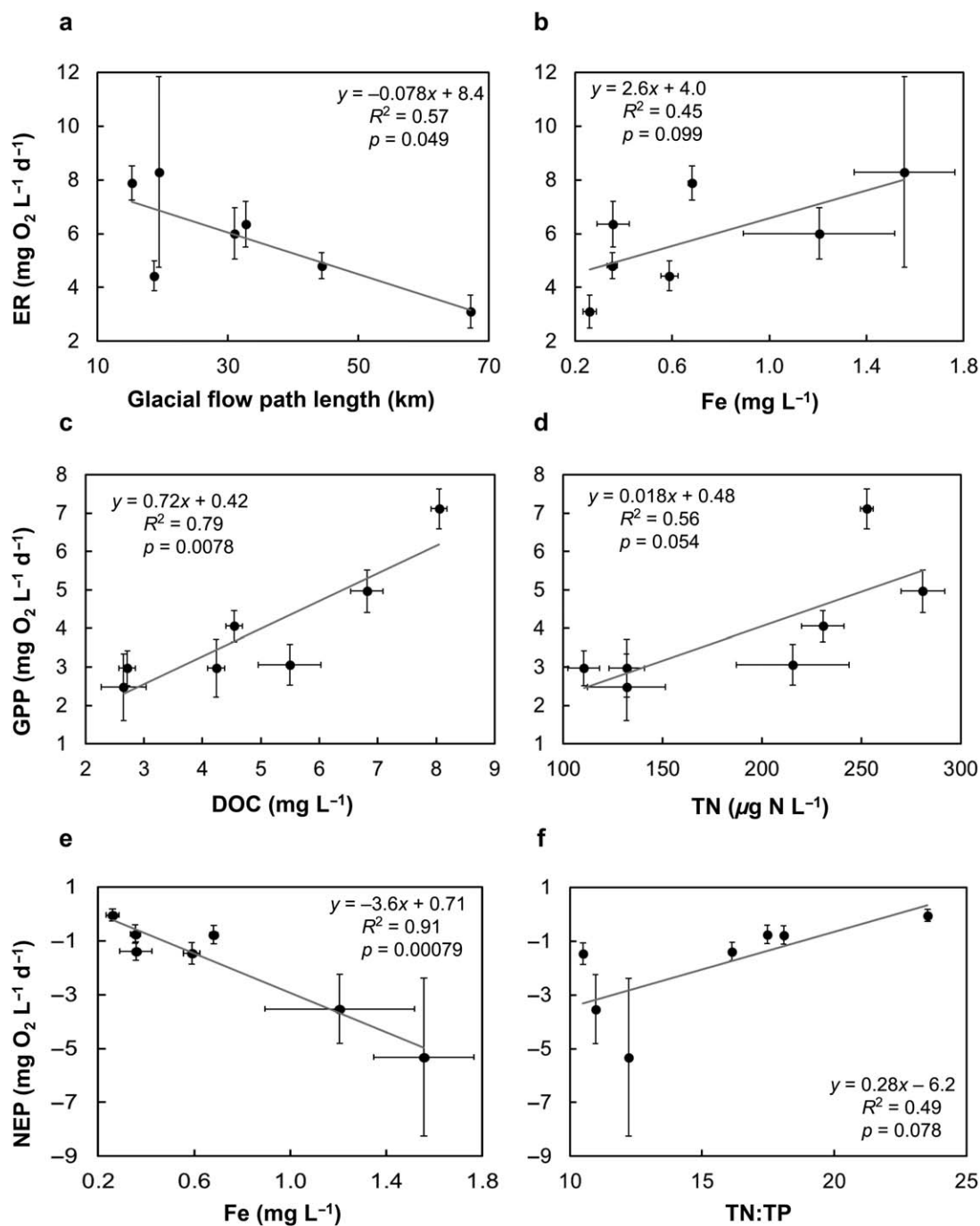
Fig. 5. Linear regressions (df = 5) between (**a**) ER and glacial flow path lengths, (**b**) ER and iron (Fe) concentrations, (**c**) GPP and DOC concentrations, (**d**) GPP and TN levels, (**e**) NEP and Fe, and (**f**) NEP and TN to TP ratios. TN : TP is reported as a molar ratio. Ecosystem metabolism estimates (ER, GPP, and NEP) were all standardized to 20°C. *p* values greater than 0.007 were not considered significant due to the false discovery rate control cutoff. Error bars represent standard error of measurements conducted at multiple sites within a pond during summer sampling.

and Scott (2008) documented that SRP peaks in Alaskan rivers when glacial runoff is at a maximum, and they postulated that the higher SRP concentrations observed in the summer in glacial watersheds may be a function of glacial weathering of calcite/apatite minerals and low in-stream phosphorus uptake. It is possible that glacial weathering is a source of SRP in the CRD, but we do not know how much it contributes to the phosphorus budget of these wetlands. It is likely that biological processes play a larger role in regulating SRP availability in most of these highly productive wetlands

than they do in glacier-fed streams where physical and hydrologic processes tend to dominate (Malard et al. 2006).

Decomposition rates were faster in ponds with higher SRP concentrations; therefore, decomposition may be limited by phosphorus or increase SRP availability due to mineralization. In a previous study conducted in CRD ponds, Tiegs et al. (2013*b*) found that the microbial decomposition rate of litter species increased with the phosphorus content of the litter, which suggests that microbial decomposers in the CRD are phosphorus-limited, at least after they are provided with a carbon source. Nevertheless, phosphorus could also be released from Fe oxide complexes as sediments become more anoxic (Gächter et al.1988), especially in glacial outwash ponds, which tend to have low DO levels at the sediment-water interface.

Faster decomposition rates could also result in higher rates of phosphorus remineralization and therefore higher SRP availability, particularly if microbial decomposers tend to be carbon-limited. In glacially influenced systems, DOC was lower (outwash ponds: 2.7–4.2 mg L^{-1}; uplifted ponds: 4.5–8.7 mg L^{-1}), macrophyte abundance was lower, and detritus was less available; these observations could explain why our cotton strips, a low-quality carbon source, were more rapidly broken down in the ponds closer to the glacier (e.g., cotton strips were often in such small pieces in outwash ponds that we could not measure tensile strength). If heterotrophic bacteria are indeed carbon-limited, then phosphorus uptake rates could be low (Currie and Kalff 1984*a*), resulting in higher SRP availability. Currie and Kalff (1984*b*) observed that heterotrophic bacteria tended to dominate SRP cycling in Lake Memphremagog, while phytoplankton obtained most of their phosphorus from organic compounds. We hypothesize that higher SRP concentrations in ponds with shorter glacial flow paths are a complex function of (1) higher P availability from low sediment redox conditions, and (2) faster decomposition and phosphorus remineralization rates due to carbon limitation of microbial decomposers.

In the CRD, heterotrophy was highest in glacially influenced ponds. The strong relationships between Fe, an element released in glacial weathering, and both ER and NEP support this pattern. Fe could impact ecosystem processes via three potential mechanisms: (1) direct limitation of aquatic primary producers or decomposers (e.g., North et al. 2007), (2) complexation with dissolved organic matter (DOM) that enhances water color (Kritzberg and Ekström 2012) and decreases light availability, and (3) precipitation or dissolution of Fe-P minerals that affect SRP availability (Jordan et al. 2008). It is unlikely that Fe is a limiting nutrient in these ponds because concentrations are two orders of magnitude higher than SRP concentrations. Similarly, light penetrated to the bottom of all the ponds, so it is unlikely that Fe impacted light availability, especially since pond Fe concentrations were not correlated with light or the light

attenuation coefficient, K_{dPAR}. Therefore, the most likely link between Fe and ecosystem processes is its ability to complex with both DOM and phosphorus. While Fe itself is unlikely to increase ER, it is possible that remineralization of Fe could track ER. For example, if microbial heterotrophs in glacial outwash ponds are carbon-limited, then DOM-Fe-P complexes could provide a carbon source for respiration, thus releasing both Fe and P to the water column. Therefore, it is possible that higher Fe and SRP concentrations could result from biological processes (i.e., decomposition and ER) as well as glacial weathering.

Although the direct link between Fe and ER in the CRD is unclear, glacial inputs of suspended sediment do provide a mechanism by which hydrology can affect ecosystem processes in these ponds. For example, the pond with the second lowest NEP, Beaver North, experienced a 1-m increase in depth when the "Dirty" Martin River, a glacial-fed stream of the Copper River, flooded this pond during August. This flood event not only increased glacial sediment, Fe levels, and turbidity, but it also greatly altered ecosystem metabolism. ER dropped dramatically from 5.2 ± 1.6 mg O_2 L^{-1} d^{-1} (mean $\pm$ SD) 1 week prior to the flood to 1.1 mg O_2 L^{-1} d^{-1} during the first day of flooding, but then rebounded to 7.9 ± 1.3 mg O_2 L^{-1} d^{-1} 1 week later while the pond was still inundated. In contrast, GPP dropped from 4.8 ± 2.8 before the flood to 0.9 mg O_2 L^{-1} d^{-1} the day of the flood, and remained depressed 1 week after (1.1 ± 0.4 mg O_2 L^{-1} d^{-1}). These observations suggest that glacial flooding of aquatic ecosystems has the ability to drastically alter ecosystem processes by decreasing light availability and therefore GPP, and also by having a shorter-term impact on ER thus decreasing NEP. Malard et al. (2006) documented similar trends whereby periphyton biomass was lower in glacially influenced channels than in clear water channels, particularly during periods of high flow.

Changes in hydrologic inputs are a form of disturbance that can dominate ecosystem processes. As glacial melt and flooding events continue to increase in frequency with warmer temperatures and higher precipitation in the near future, CRD ponds are likely to become more heterotrophic at least in the short-term. However, as glacial influence diminishes across aquatic ecosystems at high latitudes due to climate change, Milner et al. (2009) hypothesize a general increase in the diversity and production of primary producers, invertebrates, and fish, but potentially also the loss of coldwater species (e.g., Pacific salmon).

Oceanic influence on physicochemical patterns and ecosystem processes

In contrast to our expectations that sea spray would increase SO_4^{2-} availability near the ocean, SO_4^{2-} concentrations were higher in ponds farther from the ocean. Nevertheless, SO_4^{2-} is of both atmospheric and geological origin, and it

possible that sulfur cycling in the CRD is dominated by chemical weathering processes such as carbonation and the physical weathering of minerals including gypsum ($CaSO_4 \cdot 2H_2O$) and pyrite (FeS_2) (Carney et al. 2009). Therefore, if weathering is more dominant near the headwaters and SO_4^{2-}, a reactive solute, is chemically reduced as we proceed across the aquatic continuum, we might expect the observed pattern of lower SO_4^{2-} near the ocean.

Additionally, distance from the ocean or landscape position shaped light and temperature patterns. Water temperature was higher in ponds closer to the ocean likely due to differences in hydrologic source and/or residence time. For examples, ponds on the outwash plain are prone to rapid and pronounced changes in water level during the summer related to glacial melt, whereas ponds on the uplifted marsh receive water inputs from rainfall, freshwater stream inputs, and lateral flow through peat (Boggs 2001). Additionally, the amount of light penetrating the water column increased near the ocean; ponds receiving more light also had lower light attenuation coefficients suggesting that systems near the ocean exhibited lower turbidity (Koenings and Edmundson 1991).

Nutrient patterns observed in the CRD ponds were also influenced by distance from the ocean with NH_4^+ levels and DIN : SRP increasing near the ocean. The CRD patterns were the opposite of those documented in Chesapeake Bay estuaries (Jordan et al. 2008; Hartzell and Jordan 2012) likely due to different geology and ecosystem type (i.e., tidal estuaries vs. non-tidal freshwater ponds). We are unaware of other studies examining potential oceanic influence in freshwater ecosystems from a landscape perspective; therefore, mechanistic links for such patterns are not well documented. Nevertheless, we hypothesize that NH_4^+ levels are higher near the ocean in the CRD as a result of three potential mechanisms: (1) ponds near the ocean are embedded in former marine sediments containing higher nitrogen concentrations, (2) atmospheric deposition of nitrogen is greater near the ocean, and (3) nitrogen fixation by pond cyanobacteria or microorganisms associated with the roots of riparian plants is higher near the ocean. For example, in southeast Alaska, D'Amore et al. (2011) found that soils overlaying older marine sediments tended to hold more nitrogen. Second, although we are unsure of localized nitrogen deposition patterns in the CRD, interior areas of Alaska (i.e., Fairbanks, Yukon, and Denali) only received about a third of NH_4^+ and total inorganic nitrogen wet deposition compared to coastal areas of Alaska (i.e., Bristol Bay and Juneau) during 2014 (NADP-NTN 2014). Finally, high densities of *Nostoc* spp. (nitrogen-fixing cyanobacteria) have been observed in the mudflats near the Gulf of Alaska (Bryant 1991). It is also possible that riparian plants possessing symbiotic relationships with nitrogen-fixing microorganisms (i.e., *Myrica gale* and *Alnus* spp.) are more abundant toward the ocean. All of these mechanisms may contribute to the

patterns we observed in NH_4^+ levels, which in turn shaped the DIN : SRP ratios.

Ponds exhibited DIN : SRP ratios of less than 8, which suggests that primary production on the CRD is likely limited by nitrogen availability (Keck and Lepori 2012). The positive relationship between TN and GPP also supports this hypothesis. Additionally, the tight coupling of DOC and TN in these ponds suggests that decomposition is critical to internal recycling of organic matter and nutrients in these systems (cf. Bryant 1991). We also observed a positive relationship between GPP and DOC. We hypothesize that DOC in CRD ponds comes from more labile autochthonous sources (cf. terrestrial organic matter) for three reasons: (1) ponds closer to the ocean with the highest levels of DOC also tended to have higher levels of light in the water column and lower K_{dPAR}, (2) light penetrated to the bottom of all the ponds despite DOC concentrations as high as 9 mg L^{-1}, and (3) GPP was positively related with DOC, likely indicating that DOC is a product of aquatic macrophyte and possibly phytoplankton exudates (Bertilsson and Jones 2003).

Conclusions

The CRD allowed us to examine the interactive influences of both glaciers and the ocean on the freshwater wetland ponds of this northern Pacific coastal temperate landscape (O'Neel et al. 2015). Our study extends the concept of landscape position to ecosystem processes by demonstrating that landscape can shape environmental gradients over relatively short distances (*sensu* Swanson et al. 1988), and that these patterns can influence ecosystem functional processes that in turn affect environmental gradients (i.e., DOC, TN, SRP). Near the glaciers, ponds tended to display more heterotrophy, less DOC, and lower N : P ratios, whereas ponds close to the ocean were more productive with higher DOC and N : P ratios.

The concept of continua has been foundational to many areas of ecology, from plant succession to river networks. Our study extends this concept to freshwater ponds along a continuum from glaciers to ocean in a complex deltaic system. In the future, the relative importance of glacial or oceanic inputs to these continua may change through direct (e.g., hydrologic, weathering) and indirect effects (e.g., vegetation changes) as glacial melt and sea-level rise continue to accelerate (Vermeer and Rahmstorf 2009; Neal et al. 2010). Such changes in biotic communities and hydrologic processes could greatly alter the balance of ecosystem processes in both coastal and glacial freshwater ecosystems.

References

Ameel, J. J., R. P. Axler, and C. J. Owen. 1993. Persulfate digestion for determination of total nitrogen and phosphorus in low-nutrient waters. Am. Environ. Lab. **10**: 7–11.

APHA. 1995. Standard methods for the examination of water and wastewater, 19th ed. American Public Health Association.

Bergström, A.-K., P. Blomqvist, and M. Jansson. 2005. Effects of atmospheric nitrogen deposition on nutrient limitation and phytoplankton biomass in unproductive Swedish lakes. Limnol. Oceanogr. **50**: 987–994. doi:10.4319/lo.2005.50.3.0987

Bertilsson, S., and J. B. Jones. 2003. Supply of dissolved organic matter to aquatic ecosystems: Autochtonous sources, p. 3–24. *In* S. E. G. Findlay and R. L. Sinsabaugh [eds.], Aquatic ecosystems: Interactivity of dissolved organic matter. Academic Press.

Boggs, K. 2001. Classification of community types, successional sequences, and landscapes of the Copper River Delta, Alaska. General Technical Report PNW-GTR-469. U.S.D.A. Forest Service, Pacific Northwest Research Station.

Bryant, M. D. 1991. The Copper River Delta pulse study: An interdisciplinary survey of aquatic habitats. General Technical Report PNW-GTR-282. U.S.D.A. Forest Service, Pacific Northwest Research Station.

Carney, M., A. Ellis, T. Bullen, and J. Langman. 2009. Geochemistry of Yukon and Copper River tributaries, Alaska, p. 1–7. *In* World Environmental and Water Resources Congress 2009. American Society of Civil Engineers, Reston, VA.

Crusius, J., A. W. Schroth, S. Gassó, C. M. Moy, R. C. Levy, and M. Gatica. 2011. Glacial flour dust storms in the Gulf of Alaska: Hydrologic and meteorological controls and their importance as a source of bioavailable iron. Geophys. Res. Lett. **38**: L06602. doi:10.1029/2010GL046573

Currie, D. J., and J. Kalff. 1984*a*. A comparison of the abilities of freshwater algae and bacteria to acquire and retain phosphorus. Limnol. Oceanogr. **29**: 298–310. doi:10.4319/lo.1984.29.2.0298

Currie, D. J., and J. Kalff. 1984*b*. The relative importance of bacterioplankton and phytoplankton in phosphorus uptake in freshwater. Limnol. Oceanogr. **29**: 311–321. doi:10.4319/lo.1984.29.2.0311

D'Amore, D. V., N. S. Bonzey, J. Berkowitz, J. Rüegg, and S. Bridgham. 2011. Holocene soil-geomorphic surfaces influence the role of salmon-derived nutrients in the coastal temperate rainforest of Southeast Alaska. Geomorphology **126**: 377–386. doi:10.1016/j.geomorph.2010.04.014

Freymueller, J. T., H. Woodard, S. C. Cohen, R. Cross, J. Elliott, C. F. Larsen, S. Hreinsdóttir, and C. Zweck. 2008. Active deformation processes in Alaska, based on 15 years of GPS measurements, p. 1–42. *In* J. T. Freymueller, P. J. Haeussler, R. L. Wesson, and G. Ekström [eds.], Active tectonics and seismic potential of Alaska. American Geophysical Union.

Gächter, R., J. S. Meyer, and A. Mares. 1988. Contribution of bacteria to release and fixation of phosphorus in lake sediments. Limnol. Oceanogr. **33**: 1542–1558. doi:10.4319/lo.1988.33.6part2.1542

Glickman, M. E., S. R. Rao, and M. R. Schultz. 2014. False discovery rate control is a recommended alternative to Bonferroni-type adjustments in health studies. J. Clin. Epidemiol. **67**: 850–857. doi:10.1016/j.jclinepi.2014.03.012

Hartzell, J. L., and T. E. Jordan. 2012. Shifts in the relative availability of phosphorus and nitrogen along estuarine salinity gradients. Biogeochemistry **107**: 489–500. doi:10.1007/s10533-010-9548-9

Holtgrieve, G. W., D. E. Schindler, T. A. Branch, and Z. T. A'mar. 2010. Simultaneous quantification of aquatic ecosystem metabolism and reaeration using a Bayesian statistical model of oxygen dynamics. Limnol. Oceanogr. **55**: 1047–1063. doi:10.4319/lo.2010.55.3.1047

Hood, E., and D. Scott. 2008. Riverine organic matter and nutrients in southeast Alaska affected by glacial coverage. Nat. Geosci. **1**: 583–587. doi:10.1038/ngeo280

Jordan, T. E., J. C. Cornwell, W. R. Boynton, and J. T. Anderson. 2008. Changes in phosphorus biogeochemistry along an estuarine salinity gradient: The iron conveyer belt. Limnol. Oceanogr. **53**: 172–184. doi:10.4319/lo.2008.53.1.0172

Junge, C. E., and R. T. Werby. 1958. The concentration of chloride, sodium, potassium, calcium, and sulfate in rain water over the United States. J. Meteorol. **15**: 417–425. doi:10.1175/1520-0469(1958)015<0417:TCOCSP>2.0.CO;2

Keck, F., and F. Lepori. 2012. Can we predict nutrient limitation in streams and rivers? Freshw. Biol. **57**: 1410–1421. doi:10.1111/j.1365-2427.2012.02802.x

Kling, G. W., G. W. Kipphut, M. M. Miller, and W. J. O'Brien. 2000. Integration of lakes and streams in a landscape perspective: The importance of material processing on spatial patterns and temporal coherence. Freshw. Biol. **43**: 477–497. doi:10.1046/j.1365-2427.2000.00515.x

Koenings, J. P., and J. A. Edmundson. 1991. Secchi disk and photometer estimates of light regimes in Alaskan lakes: Effects of yellow color and turbidity. Limnol. Oceanogr. **36**: 91–105. doi:10.4319/lo.1991.36.1.0091

Kratz, T., K. Webster, C. Bowser, J. Maguson, and B. Benson. 1997. The influence of landscape position on lakes in northern Wisconsin. Freshw. Biol. **37**: 209–217. doi:10.1046/j.1365-2427.1997.00149.x

Kritzberg, E. S., and S. M. Ekström. 2012. Increasing iron concentrations in surface waters – a factor behind brownification? Biogeosciences **9**: 1465–1478. doi:10.5194/bg-9-1465-2012

Lake Ecosystem Restoration New Zealand. 2016. B3 and data standardizer. https://www.lernz.co.nz/tools-and-resources/b3

Malard, F., U. Uehlinger, R. Zah, and K. Tockner. 2006. Flood-pulse and riverscape dynamics in a braided glacial river. Ecology **87**: 704–716. doi:10.1890/04-0889

Milner, A. M., L. E. Brown, and D. M. Hannah. 2009. Hydroecological response of river systems to shrinking glaciers. Hydrol. Process. **23**: 62–77. doi:10.1002/hyp.7197

Murphy, J., and J. P. Riley. 1962. A modified single solution method for the determination of phosphate in natural

waters. Anal. Chim. Acta **27**: 31–36. doi:10.1016/S0003-2670(00)88444-5

NADP-NTN. 2014. NADP-NTN report of wet deposition data. National Atmospheric Deposition Monitoring Program/ National Trends Network.

Neal, E. G., E. Hood, and K. Smikrud. 2010. Contribution of glacier runoff to freshwater discharge into the Gulf of Alaska. Geophys. Res. Lett. **37**: L06404. doi:10.1029/2010GL042385

North, R. L., S. J. Guildford, R. E. H. Smith, S. M. Havens, and M. R. Twiss. 2007. Evidence for phosphorus, nitrogen, and iron colimitation of phytoplankton communities in Lake Erie. Limnol. Oceanogr. **52**: 315–328. doi:10.4319/lo.2007.52.1.0315

O'Neel, S., and others. 2015. Icefield-to-ocean linkages across the northern Pacific coastal temperate rainforest ecosystem. BioScience **65**: 499–512. doi:10.1093/biosci/biv027

Parkhill, K. L., and J. S. Gulliver. 1999. Modeling the effect of light on whole-stream respiration. Ecol. Modell. **117**: 333–342. doi:10.1016/S0304-3800(99)00017-4

R Development Core Team. 2016. R: a language and environment for statistical computing. Available from: http://www.R-project.org

Read, J. S., K. C. Rose, L. A. Winslow, and E. K. Read. 2015. A method for estimating the diffuse attenuation coefficient (KdPAR) from paired temperature sensors. Limnol. Oceanogr.: Methods **13**: 53–61. doi:10.1002/lom3.10006

Risser, P. G. 1987. Landscape ecology: State of the art, p. 3–14. *In* M. G. Turner [ed.], Landscape heterogeneity and disturbance. Springer.

Rose, K. C., L. A. Winslow, J. S. Read, E. K. Read, C. T. Solomon, R. Adrian, and P. C. Hanson. 2014. Improving the precision of lake ecosystem metabolism estimates by identifying predictors of model uncertainty. Limnol. Oceanogr.: Methods **12**: 303–312. doi:10.4319/lom.2014.12.303

Sadro, S., C. E. Nelson, and J. M. Melack. 2011. The influence of landscape position and catchment characteristics on aquatic biogeochemistry in high-elevation lake-chains. Ecosystems **15**: 363–386. doi:10.1007/s10021-011-9515-x

Schroth, A. W., J. Crusius, F. Chever, B. C. Bostick, and O. J. Rouxel. 2011. Glacial influence on the geochemistry of riverine iron fluxes to the Gulf of Alaska and effects of deglaciation. Geophys. Res. Lett. **38**: L16605. doi:10.1029/2011GL048367

Simó, R., and C. Pedrós-Alió. 1999. Role of vertical mixing in controlling the oceanic production of dimethyl sulphide. Nature **402**: 396–399. doi:10.1038/46516

Solomon, C. T., and others. 2013. Ecosystem respiration: Drivers of daily variability and background respiration in lakes around the globe. Limnol. Oceanogr. **58**: 849–866. doi:10.4319/lo.2013.58.3.0849

Solórzano, L. 1969. Determination of ammonia in natural waters by the phenolypochlorite method. Limnol. Oceanogr. **14**: 799–801. doi:10.4319/lo.1969.14.5.0799

Soranno, P. A., and others. 1999. Spatial variation among lakes within landscapes: Ecological organization along lake chains. Ecosystems **2**: 395–410. doi:10.1007/s100219900089

Steinman, A. D., G. A. Lamberti, and P. R. Leavitt. 2006. Biomass and pigments of benthic algae, p. 357–380. *In* F. R. Hauer and G. A. Lamberti [eds.], Methods in stream ecology. Academic Press.

Swanson, F. J., T. K. Kratz, N. Caine, and R. G. Woodmansee. 1988. Landform effects on ecosystem patterns and processes. BioScience **38**: 92–98. doi:10.2307/1310614

Thilenius, J. F. 1995. Phytosociology and succession on earthquake-uplifted coastal wetlands, Copper River Delta, Alaska. PNW-GTR-346. U.S.D.A. Forest Service, Pacific Northwest Research Station.

Tiegs, S. D., S. D. Langhans, K. Tockner, and M. O. Gessner. 2007. Cotton strips as a leaf surrogate to measure decomposition in river floodplain habitats. J. North Am. Benthol. Soc. **26**: 70–77. doi:10.1899/0887-3593(2007)26[70:CSAALS]2.0.CO;2

Tiegs, S. D., J. E. Clapcott, N. A. Griffiths, and A. J. Boulton. 2013*a*. A standardized cotton-strip assay for measuring organic-matter decomposition in streams. Ecol. Indic. **32**: 131–139. doi:10.1016/j.ecolind.2013.03.013

Tiegs, S. D., S. A. Entrekin, G. H. Reeves, D. Kuntzsch, and R. W. Merritt. 2013*b*. Litter decomposition, and associated invertebrate communities, in wetland ponds of the Copper River Delta, Alaska (USA). Wetlands **33**: 1151–1163. doi:10.1007/s13157-013-0470-5

Turner, M. G. 2005. Landscape ecology: What is the state of the science? Annu. Rev. Ecol. Evol. Syst. **36**: 319–344. doi:10.1146/annurev.ecolsys.36.102003.152614

U.S. Geological Survey. 1990. Largest rivers in the United States. https://pubs.usgs.gov/of/1987/ofr87-242/

U.S. Geological Survey. 2013. USGS National Hydrography Dataset Flowline and Waterbody features. https://nhd.usgs.gov/

Vannote, R. L., G. W. Minshall, K. W. Cummins, J. R. Sedell, and C. E. Cushing. 1980. The river continuum concept. Can. J. Fish. Aquat. Sci. **37**: 130–137. doi:10.1139/f80-017

Vermeer, M., and S. Rahmstorf. 2009. Global sea level linked to global temperature. Proc. Natl. Acad. Sci. USA. **106**: 21527–21532. doi:10.1073/pnas.0907765106

Vitousek, P. M., J. D. Aber, R. W. Howarth, G. E. Likens, P. A. Matson, D. W. Schindler, W. H. Schlesinger, and D. G. Tilman. 1997. Human alteration of the global nitrogen cycle: Sources and consequences. Ecol. Appl. **7**: 737–750. doi:10.1890/1051-0761(1997)007[0737:HAOTGN]2.0.CO;2

Winslow, L. A., J. A. Zwart, R. D. Batt, H. A. Dugan, R. I. Woolway, J. R. Corman, P. C. Hanson, and J. S. Read. 2016. LakeMetabolizer: An R package for estimating lake metabolism from free-water oxygen using diverse statistical models. Inland Waters **6**: 622–636. doi:10.5268/IW-6.4.883

Conflict of Interest

None declared.